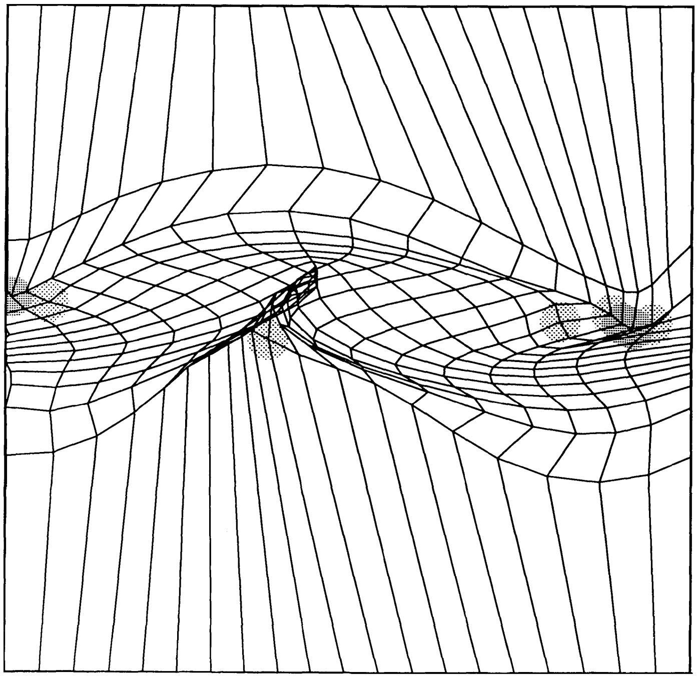

2e

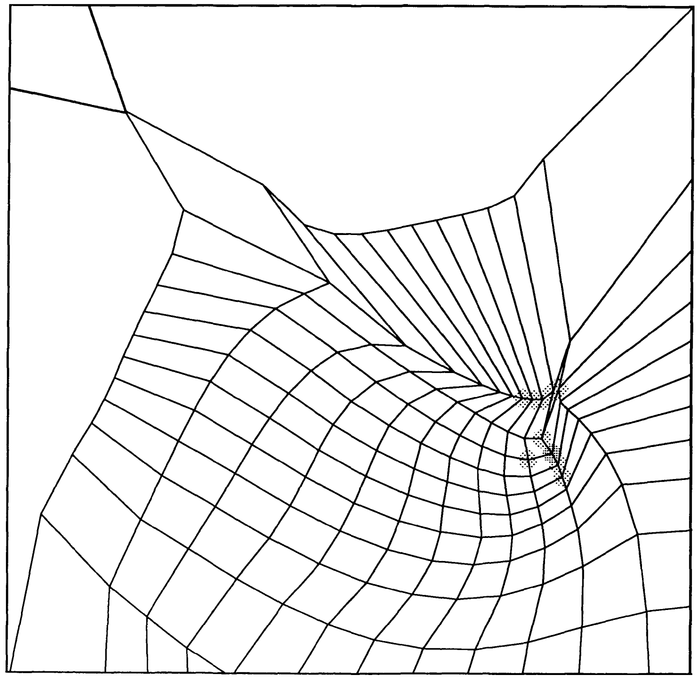

F2f

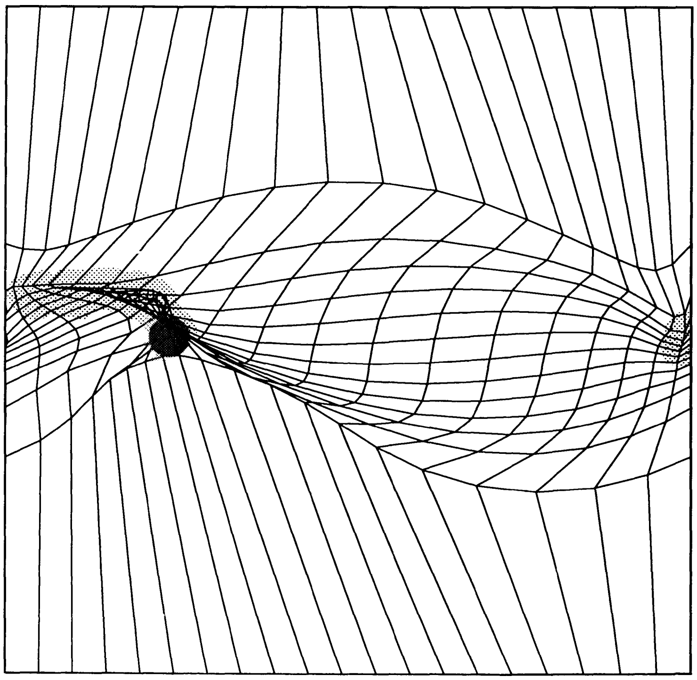

)„f—(f

)ξ,f—2—Continued

MllMmTi ıdT MSSf ekiMfokicf oSfiMfnTs eki BecomT)ξ⁻ en ndkqi neisT denisfooSTndT mTcekiqdTmTTfoTs nsesmTien ikn ei TinT.

ıdT iMciT fs TiTmcunTfoTMSdTSeic iMciT es mTfoMrM fki, qMnsMfosofoMFTSei TcmM fiqdT kqTm kU dT HEkmTi bmsT $(J \times \boldsymbol{B})$ $\boldsymbol{v}$ over space and time. The results proved somewhat unreliable since the magnitude F

F

— F could increase by as much as an order of magnitude, indicating that the true evolution was not accurately followed. Apparently the evolution of the kink follows a near-equilibrium path, and small deviations from this path give rise to much larger relative errors in F (Nevertheless the path deviations caused by choice of a large time step did not compromise the overall course of the kink evolution.) Since we generally chose as large a time step as possible to reduce the (considerable) computation time, our results f r energy release were overestimates, but it was still clear that the fgure was quite small - less than - 5% of the total magnetic energy. We also experimented with calculating changes in magnetic energy by integrating $\boldsymbol{B}$

F

P F $\boldsymbol{B}$

x- and y-directions, and seven in the z-direction. The initial perturbation was a multiple of the most slowly decaying linear normal mode, and was calculated using the methods of Craig 5BT,≠(1988) on an identical computational grid.

Figure 3 shows that both $\phi_{-\neq}$ and $\xi_{-\neq}$ decay to zero as expected. The decay is rather slow since the most slowly decaying mode is very close to marginal stability, and restoring forces are very weak. Figure 3 also shows a graph of $\phi_{-\neq}$ against t

$\boldsymbol{A}$

)r k. J

decreases rapidly, indicating a settling-down period as the initial perturbation relaxes to near equilibrium; then <-,- increases gradually as the kink instability gathers momentum. In theory <-,- should tend to zero again as the new equilibrium is approached, but the onset of current sheets and lack

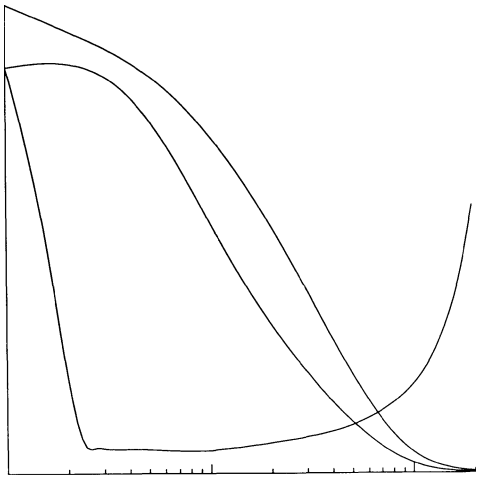

FIG. 3.—Graphs of ϕ_{max} (the maximum angle between $\boldsymbol{B}$ and $\boldsymbol{J}$) and ξ_{max} (the maximum mesh displacement from Gold-Hoyle equilibrium) against t for stable and unstable flux tubes. Note that the time scale is logarithmic.

of resolution means that the angles cannot be calculated with sufficient accuracy.

d) Nonlinear Interactions

Any physical initial perturbation will consist of a superposition of many eigenmodes, and it is important to understand whether the initial presence of other modes interferes with the development of $\boldsymbol{\xi}_1$. We experimented with two initial perturbations described by analytic formulae. The first was a simple "bend," given by the formula

$$\boldsymbol{\xi}_a = \cos\left(\frac{\pi z}{2l}\right)\cos\left(\frac{\pi x}{2a}\right)\cos\left(\frac{\pi y}{2a}\right)\hat{\boldsymbol{x}} .$$

The second was a helical-kink displacement given by the formula

$$\boldsymbol{\xi}_b = [(f(r)\cos\psi\hat{\boldsymbol{r}} - g(r)\sin\psi\hat{\theta} + rg(r)\sin\psi\hat{z}]\cos\left(\frac{\pi z}{2l}\right),$$

in cylindrical polar coordinates (r, θ, z), where

$$\psi = \theta - kz\ , \quad f(r) = \begin{matrix}(1 - r^2/a^2)\\(1 + r^2)\end{matrix}\ , \quad g(r) = \frac{f(r)(1 - r^2)}{1 + r^2}\ .$$

(To ensure that $\boldsymbol{\xi}_b = 0$ on the boundaries $|x|, |y| = a$ the function f was defined to be zero for $r \geq a$.) The displacement $\boldsymbol{\xi}_b$ was designed to mimic the form of the most unstable $m = 1$ mode for the infinite Gold-Hoyle flux tube, as described by Sneyd and Craig (1988), but multiplied by the cosine factor to ensure $\boldsymbol{\xi}_b = 0$ on the endplates $|z| = l$. The wavenumber k was chosen to be 0.5, as this value seemed to maximize the initial $\boldsymbol{\xi}_1$-component c_1.

Figure 4*a* shows the growth of the most unstable mode (as measured by the coefficient c_1) for instabilities initiated by multiples of the above displacements. In both cases the maximum initial mesh displacement is 0.2. With the $\boldsymbol{\xi}_a$ displacement, c_1 increases slightly, decays to zero, and then begins to grow rapidly in the negative sense. In the $\boldsymbol{\xi}_b$ case the initial value of c_1 is smaller (somewhat surprising since this form of disturbance was purposely designed to mimic the most unstable mode); c_1 again grows briefly, then decreases, but eventually begins to grow slowly again. In both cases the coefficient c_n (the mean square measure of displacement in modes $\boldsymbol{\xi}_2, \boldsymbol{\xi}_3 \ldots$) is almost exactly unity, indicating that $\boldsymbol{\xi}_1$ comprises a very small proportion of the total displacement. Figure 4*b* shows a mesh cross-section during the evolution of the $\boldsymbol{\xi}_a$ displacement, which indicates that most of the residual displacement is in the outer regions of the flux tube, where the magnetic field and restoring forces are weak.

Note that in Figure 4*a* the time coordinate is pseudo time. Since nonlinear interactions are important it is not possible to make a simple comparison with Alfvén time. However, we can generally conclude that the presence of other eigenmodes seems to prevent early growth of the most unstable mode.

IV. CONCLUSIONS

We have used a magnetic relaxation technique to study the nonlinear evolution of three-dimensional ideal MHD insta-

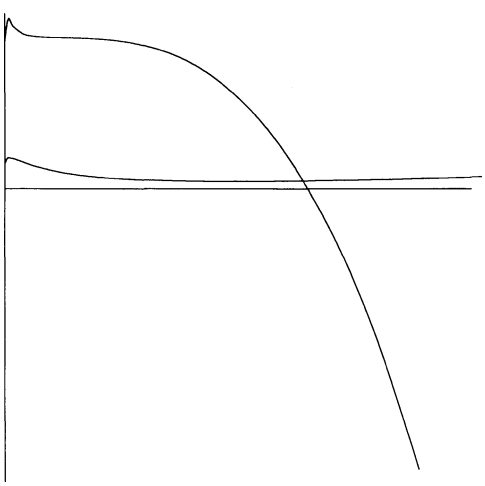

FIG. 4*a*

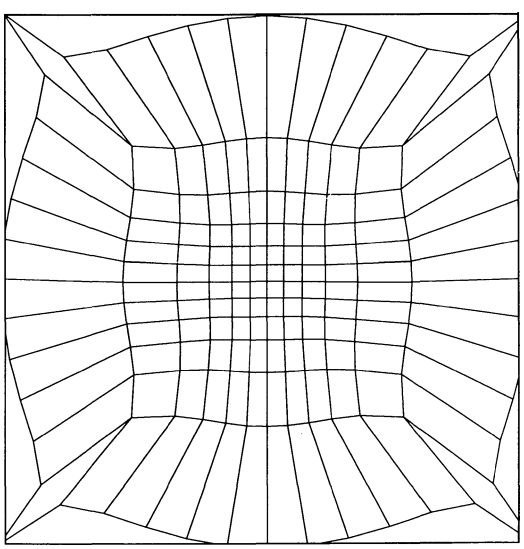

FIG. 4*b*

FIG. 4.—(*a*) Graphs of c_1 against t for the initial displacements $\boldsymbol{\xi}_a$ and $\boldsymbol{\xi}_b$. (*b*) Mesh section $Z = 0$ for $\boldsymbol{\xi}_a$ at $t = 1300$.

bilities. Since the relaxation method is Lagrangian, using a grid of fluid particle positions as basic variables, the evolution of small length-scale structures can be represented more accurately than by means of a fixed (Eulerian) mesh. The scheme preserves magnetic flux and therefore magnetic helicity identically. It incorporates an ADI technique to integrate the evolution equations forward in time, so that relatively large time steps may be taken unhindered by numerical stability restrictions; in practice typical time steps may be three orders of magnitude beyond the explicit stability limit.

To gain insight into nonlinear processes in coronal loops, we have applied the Lagrangian relaxation method to the kink instability in an unstable, line-tied, Gold-Hoyle flux tube. Nonlinear forces accelerate the kink quite strongly and are important even in the early stages of development. This could be anticipated since linear theory predicts forces of order $\lambda\xi$, where λ, the eigenvalue of the most unstable linear mode, $=2.4 \times 10^{-4}$ in our chosen example. The strongest nonlinear forces are of order ξ^3, and become equally important when $\xi = O(10^{-2})$—i.e., at quite modest amplitudes. Eventually the kinked flux tube reaches a new equilibrium which appears to contain current sheets.

Current sheets appear mostly near the tube ends. They are formed by the close approach of magnetic surfaces, partly due to compression, and partly to shearing. It should be emphasized that the maximum compression factor in our calculation is ~ 20, while in a coronal loop compression factors of at least 10^3 would be necessary if plasma pressure were to become comparable with magnetic pressure. Moreover, a current sheet can be formed by means of pure shear, even in an incompressible flow, so we would not expect plasma pressure to prevent current sheets.

An important conclusion is that little magnetic energy (somewhat less than 5% of the total available) is released in the ideal MHD phase of development. However, with the appearance of current sheets, more devastating resistive instabilities will take effect. The role of ideal MHD can therefore be seen as driving the field toward a singular configuration, with length scales small enough to cause magnetic reconnection and violent energy release.

Our studies of nonlinear interactions indicate that the most unstable mode (in linear theory) may be damped in the presence of other modes. Real coronal loops are subject to continual random perturbations, which could keep the kink instability suppressed over long periods, thus explaining the observed longevity of the loops. Another possibility, which follows from the inherent weakness of the kink, is that its nonlinear development could be suppressed by neighboring stable loops in the active region assemblage. However, if isolated loops do exist and these are driven into instability by some mechanism—say by photospheric twisting of the footpoints—then the field will distort and release magnetic energy relatively slowly over, say, at least 10^2 Alfvén times. Either way, since the ideal MHD phase is effective mainly in driving the field toward a configuration involving current sheets, it remains for resistive effects to release the bulk of the stored magnetic energy.

We gratefully acknowledge support from the New Zealand University Grants Committee, and University of Waikato Research Committee, for the purchase of the Microvax II computers used for our computations.

APPENDIX

EIGENVALUES OF M

We note first that M can be written in the form

$$M = -B^2 k^2 P_B P_k \,, \tag{A1}$$

where the matrix P_B projects any vector onto the plane normal to $\boldsymbol{B}$, and similarly for P_k. We now consider the eigenvalues of $P_B P_k$.

Obviously $\boldsymbol{k}$ is an eigenvector with corresponding eigenvalue 0. Furthermore a vector along the line of intersection of the planes

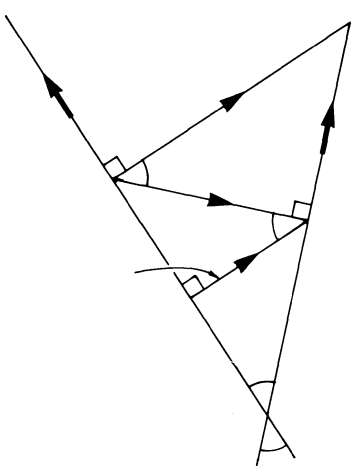

FIG. 5.—Geometrical construction for finding eigenvalue of $P_B P_k$.

normal to $\boldsymbol{k}$ and $\boldsymbol{B}$ is invariant under both projection operations and is therefore an eigenvector with corresponding eigenvalue 1. Since $P_B P_k$ is real and eigenvalues must occur in complex conjugate pairs, it follows that the third eigenvector is also real, say λ. The general solution for $\boldsymbol{x}$ of $P_k \boldsymbol{x} = \boldsymbol{y}$ is $\boldsymbol{x} = \boldsymbol{y} + \alpha \boldsymbol{k}$, where α is any scalar, so the solution of the eigenvalue equation

$$P_B P_k \boldsymbol{x} = \lambda \boldsymbol{x} \quad \text{is} \quad \boldsymbol{x} = \lambda \boldsymbol{x} + \alpha \boldsymbol{k} + \beta \boldsymbol{B} \,. \tag{A2}$$

Thus, either $\lambda = 1$ which implies that $\boldsymbol{B}$ and $\boldsymbol{k}$ are parallel, in which case the eigenvalue 1 is repeated, having an eigenspace of dimension 2. Alternatively if $\lambda \neq 1$ then $\boldsymbol{x}$ lies in the plane of $\boldsymbol{B}$ and $\boldsymbol{k}$. It also follows from equation (A2) that $\boldsymbol{x}$ must be perpendicular to $\boldsymbol{B}$, and the geometric construction in Figure 5 shows that $\lambda = \cos^2 \theta$, where θ is the angle between $\boldsymbol{B}$ and $\boldsymbol{k}$.

From equation (A1) the eigenvalues of M are therefore

$$\{-B^2k^2,\ 0,\ -B^2k^2 \cos^2 \theta\} \,.$$

REFERENCES

Anzer, U. 1968, *Solar Phys.*, **3**, 298.
Arnol'd, V. I. 1974, in *Proc. Summer School in Differential Equations* (Erevan: Armenian SSR Academy of Science).
Bajer, K. 1989, Ph.D. thesis, University of Cambridge.
Chodura, R., and Schlüter, A. 1981, *J. Comput. Phys.*, **41**, 68.
Craig, I. J. D., McClymont, A. N., and Sneyd, A. D. 1988, *Ap. J.*, **335**, 441.
Craig, I. J. D., and Sneyd, A. D. 1986, *Ap. J.*, **311**, 451.
———. 1988, *Comput. Math. Appl.*, **16**, No. 4, 341.
———. 1990, *Comput. Math. Appl.*, to appear.
Foote, B. J., and Craig, I. J. D. 1990, *Ap. J.*, **350**, 437.
Hood, A. W., and Priest, E. R. 1981, *Geophys. Ap. Fluid Dyn.*, **17**, 297.
Moffatt, H. K. 1985, *J. Fluid Mech.*, **154**, 493.
Raadu, M. A. 1972, *Solar Phys.*, **22**, 425.
Parker, E. N. 1972, *Ap. J.*, **174**, 499.
———. 1986, *Geophys. Ap. Fluid Dyn.*, **34**, 243.
Sneyd, A. D. 1989, *Geophys. Ap. Fluid Dyn.*, in press.
Sneyd, A. D., and Craig, I. J. D. 1988, *Ap. Space Sci.*, **151**, 265.
Syrovatski, S. I. 1971, *Soviet Phys.—JETP Letters*, **33**, 933.
Tsinganos, K. C., Distler, J., and Rosner, R. 1984, *Ap. J.*, **278**, 40a.
van Ballegooijen, A. A. 1985, *Ap. J.*, **298**, 421.
———. 1988, *Geophys. Ap. Fluid Dyn.*, **41**, 181.
Velli, M., Einaudi, G., and Hood, A. W. 1990, *Ap. J.*, **350**, 428.
Yang, W. H., Sturrock, P. A., and Antiochos, S. K. 1986, *Ap. J.*, **309**, 383.

I. J. D. Craig and A. D. Sneyd: University of Waikato, Private Bag, Hamilton, New Zealand